Infrared small target detection based on modified local entropy and EMD

He Deng (邓 鹤), Jianguo Liu (刘建国), and Zhong Chen (陈 忠)*

Institute for Pattern Recognition and Artificial Intelligence,
Huazhong University of Science and Technology, Wuhan 430074, China
**E-mail: henpacked@163.com*

Received March 18, 2009

Image entropy and empirical mode decomposition (EMD) are effective methods for target detection. EMD algorithm is a powerful tool for adaptive multiscale analysis of nonstationary signals. A new technique based on EMD and modified local entropy is proposed in small target detection under sea-sky background. With the EMD algorithm, it is valid to estimate the background and get the target image by removing the background from the original image and segmenting the target based on the modified local entropy method. The data analysis and experiments show the validity of the proposed algorithm.

OCIS codes: 100.2000, 100.3008.
doi: 10.3788/COL20100801.0024.

There are many researches on the detection, identification, and tracking applications of small targets[1,2]. The main difficulty of small target detection is that there is no shape, size, texture and other information can be used. In most cases, the target is supposed either darker or brighter than its immediate adjacent background, thus a possibility is provided to detect small infrared target.

Since the concept of information entropy was introduced to image processing, it has aroused broad applications in image recovery, edge detection, target detection, image matching, and so on. In the relatively uniform texture characteristics of the background, it provides a possible way to detect the target because of the emergence of the target, damaging the image texture characteristics. For background images, the entropy should be identified because its texture characteristics are definitive. When a target appears in the images, it destructs the characteristics of the image texture, then the entropy changes. Small target contributes little to the whole image entropy in the infrared image, and it may be submerged by the noise, so it offers very little help in detection. But in the local window, the gray change caused by a small target may lead to greater local entropy changes, so it is easy to detect the existence of a small target. The algorithm based on local entropy[3] may bring the appearance of target range diffusion and result in false detection. A revised method, entropy rise method, was proposed in Ref. [4]. Unfortunately, this method is not always accurate. Therefore, a modified local entropy method is proposed in this letter.

However, in the complex background of infrared image, the features of both target and background are generally nonseparable in the original image space. It is difficult for traditional detection algorithms to work in the original image space, and it is not accurate enough to detect small targets by relying only on the modified local entropy method proposed here.

In order to overcome these difficulties and improve the testing results, a novel method to detect small targets under complex sea-sky background is proposed. The method is based on the empirical mode decomposition (EMD) and modified local entropy. EMD algorithm was initially proposed by Huang *et al.* in 1998[5]. The algorithm can extract intrinsic mode function (IMF) by decomposing the local energy associated with the intrinsic time scales of the signal itself. So it is adaptive and can depict the time-frequency characteristics of the signal. The method proposed in this letter is similar to wavelet transformation. The process of detecting small targets may be divided into four steps: firstly, decompose the original image into IMFs based on EMD algorithm; secondly, reconstruct the approximate IMFs into a background image; thirdly, obtain an image mainly including target and noise point by using background image subtracted from the original image; finally, choose a self-adaptive threshold based on the modified local entropy to segment the image.

In an infrared image under sea-sky background, due to the pixel non-uniformity of response of the infrared image, the atmospheric transmitting and scattering, the complex background containing large area of cloud and ocean waves and so on, the background in infrared scene shows significantly undulant spatial correlation between each pixel and its surroundings, while in frequency domain it lies in low frequency band and belongs to low frequency interferer for target detection[6,7]. Furthermore, it is important to note that noise comes from the infrared sensor and the background as well. Because of the effects of inherent sensor noise and the natural factors such as weather, wind, sun light, etc., there exist some high gray regions in the infrared image as complicated cloud edge, irregular sun light spot, etc. All of these and the targets can be considered as homogeneous region and fall in high frequency band, belonging to a high frequency interferer for target detection.

Basis decomposition techniques such as Fourier decomposition and wavelet decomposition have been used to analyze real-world signals. The main drawback of these approaches is that the basic functions are fixed, and do not necessarily match the varying nature of signals. Re-

cently EMD method has been proposed as a new tool for data analysis. It is a signal processing technique particularly suitable for nonlinear and non stationary series[5]. This technique performs a time-adaptive decomposition of a complex signal into elementary but almost orthogonal components that do not overlap in frequency.

EMD can break down a signal to a series of zero-mean functions, i.e., IMFs, which satisfy two conditions. These two conditions are also the criteria for sifting processes and for its stopping. There are two steps in each sifting process: 1) construct upper and lower envelopes by connecting all maxima and all minima with cubic splines; 2) subtract the mean of the upper and lower envelopes from the original signal to get a component. The sifting process should usually be applied several times because the components created by only one sifting process can hardly satisfy all the requirements of an IMF. Once an IMF is created, the same procedure will then be applied on the residual of the signal to obtain the next IMF. The later an IMF is, the lower its frequency will be. The decomposition will stop when no more IMFs can be created or the residual is less than a predetermined small value. While modes and residuals can intuitively be given a "spectral" interpretation, it is worth stressing the fact that, in general cases, their high-frequency versus low-frequency discrimination applies only locally and corresponds by no way to a predetermined subband filtering (e.g., in a wavelet transform).

As far as the one-dimensional (1D) case is concerned, studies have been carried out to show the similarities of EMD with selective filter bank decompositions[8]. Its efficiency for signal denoising has also been shown[9]. These interesting aspects of the EMD motivate the extension of this method to two-dimensional (2D) signals.

The basis of 1D EMD is the construction of some IMFs that are constructed through a sifting process. A 1D sifting process is an iterative procedure depending on the following four important problems: 1) how to define the extremal points of signal; 2) the choice of interpolation method to interpolate those extremal points from the first step; 3) how to define a stopping criterion that ends the procedure; 4) the method dealing with boundary data of the image. The process of 2D EMD is similar to that of 1D EMD, but for 2D EMD, those four problems will be more crucial.

For the first problem mentioned above, assuming that $f[m,n]$ is an $M\times N$ image, we use the definition of extreme as follows[10]: $f[m,n]$ is a maximum (minimum) if it is larger (lower) than the value of f at the eight nearest neighbors of $[m,n]$.

As far as the interpolation is concerned, several techniques have been proposed, for instance, radial basis functions such as thin-plate splines. These methods require the resolution of time-consuming optimization problems, which makes them hard to exploit, especially in a noisy context. Since Delaunay triangulation has good fitting characteristics for scattered or arbitrary data points, we first dissect the maximum (minimum) of the image matrix into a series of triangles based on Delaunay triangulation, and then interpolate each triangle by the piecewise cubic spline to form upper and lower envelopes of the image.

We adopt a 2D EMD based on Delaunay triangulation and a fixed number of iterations to build IMFs. The above method is similar to the method in Ref. [10]. The major advantage of the proposed method over existing ones is that it takes into account the geometry while preserves a low computational cost.

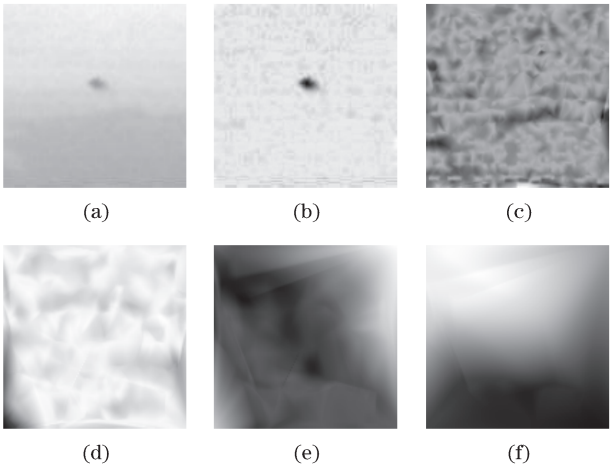

Fig. 1. (a) Original target image; (b)−(e) IMFs; (f) residue figure.

The boundary handling in 2D EMD is more difficult than that in 1D EMD, but the general approach applies only to a certain type of one or more of the borders. In addition, there is no theoretical proof to testify which approach is better. In this letter, we deal with boundary issue based on the mirror reflection of image data.

Though the method based on EMD is similar to wavelet transformation, it can decompose the image into some IMFs and the residue, in other words, it can decompose the image into different frequencies, with the first IMF denoting the highest frequency, the second IMF denoting the second highest frequency, and so on. We want to extract the target from the infrared image under sea-sky background shown in Fig. 1(a) according to our method. Figures 1(b)−(e) show four IMFs, and Fig. 1(f) depicts the decomposition residue. Figure 1(f) contains the information background naturally, and thus it can be used as the estimation of the background.

Target detection algorithms have been steadily improving, whereas many of them fail to work robustly during the applications involving changing backgrounds that are frequently encountered.

Let $F=[f(x,y)]_{M\times N}$ be an image of size $M\times N$, where $f(x,y)$ is the gray value at (x,y); $f(x,y)\in G_L=\{0,1,\cdots,L-1\}$, G_L is the set of gray levels. The definition of entropy is described as

$$\begin{cases} H_f = -\sum\limits_{i=1}^{M}\sum\limits_{j=1}^{N} p_{ij}\log p_{ij} \\ p_{ij} = f(i,j) \Big/ \sum\limits_{i=1}^{M}\sum\limits_{j=1}^{N} f(i,j), \end{cases} \tag{1}$$

where H_f is the image entropy and p_{ij} is the gray distribution. Assumed that $M\times N$ is the size of a local window of image, H_f is then called the local entropy of image.

When an infrared small target is detected based on local entropy[3], the calculation of the entropy is simplified

as

$$H \approx -\sum_{i=1}^{M}\sum_{j=1}^{N} p_{ij}\,(p_{ij}-1) = 1 - \sum_{(i,j)\in(M,N)} p_{ij}^2 \quad . \tag{2}$$

For further simplification, we assume that[4]

$$H_f = 1 - H = \sum_{(i,j)\in(M,N)} p_{ij}^2 \quad . \tag{3}$$

In the relatively homogeneous gray-scale spaces, H_f has a less value; in the large discrete areas, it has a greater value. Its value, although reflecting the degree of dispersion of the image grey, is exactly the opposite of the "entropy" original nature. In order to facilitate the expression, it is still called "local entropy".

It has been denoted that the algorithm proposed in Ref. [3] may lead to target range diffusion and false detection[4]. So a resoluble algorithm is put forward which is called the entropy rise method.

We suppose that the target is in position 0 and the background is uniform (Fig. 2(a)), and H_9 denotes the local entropy of a 3×3 small neighborhood (a 9-pixel point) as described in Eq. (1) within the image. If the center point is removed, a new local map (an 8-pixel point) is formed with the neighborhood points (Fig. 2(a), positions 1−8). A new local entropy is calculated as described in Eq. (1) and denoted as H_8. Then a new local entropy is defined as

$$H_z = H_9 - H_8. \tag{4}$$

H_z was the growth scope of local entropy, and it might be referred to as "entropy rise".

Assumed that there is no target in the uniform background, H_9 is equal approximately to H_8, in other words, H_z is approximately 0. But if a target is located in the center point, owing to the appearance of the target, the dispersion of 3×3 scope will increase and be removed from the center point, and the dispersion reduces. So a conclusion can be drawn that there exists a target if H_z is not equal to 0[4].

The entropy rise method in Ref. [4] seems somewhat true, but in the following sample, it may lead to an inappropriate conclusion. In Fig. 2, if we appoint 4 to the gray value of position 0, and 2 to the other positions (Fig. 2(b)), we can say that the position 0 is the point of target out of question. We can compute H_9, H_8, and H_z according to Ref. [4] (see Table 1), but if we appoint 2 to the gray value of all positions (Fig. 2(c)), we will find that there is no target in the local window. We can also compute H_9^*, H_8^*, and H_z^* according to Ref. [4] (see Table 1). In Table 1, we modify H_z as its absolute value. It can be seen that the value of H_z in Fig. 2(b) is smaller than that in Fig. 2(c). However, there exists a target in Fig. 2(b), not in Fig. 2(c), so the method in Ref. [4] is not accurate to some degree. Someone may say that the revised expression of "entropy rise" causes the inaccuracy. Now if we appoint 0 to the grey value of position 0, and 2 to the other positions (Fig. 2(d)),we will find that there exists a darker target in the image, but the value of H_z is 0 and there seems to be no target in the image according to Ref. [4].

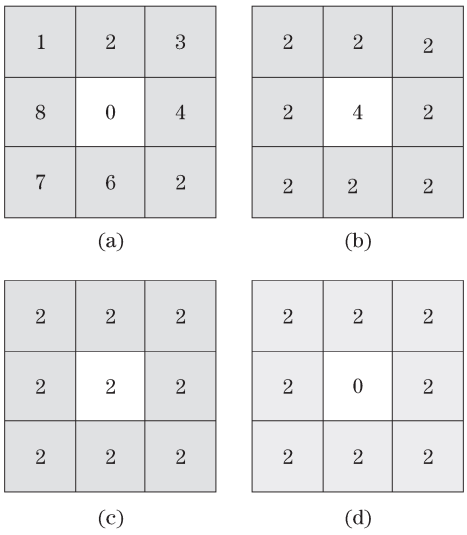

Fig. 2. A target point and its neighborhood points.

Table 1. Values of Entropy for Figs. 2(b)−(d)

	H_9	H_8	H_z
Fig. 2(b)	0.120	0.125	0.005
Fig. 2(c)	0.111	0.125	0.014
Fig. 2(d)	0.125	0.125	0

The same conclusion can be drawn from Figs. 3−7. We assume that $I(m,n)$ is an image and the size of it is 12×12, (m,n) denotes the coordinates of the image points. Similarly, assume that the value of $I(6,6)$ is 4 and others is 2. Figure 3 is an original image and Fig. 4 is the result by the method of Ref. [3]. We can find it causes target range diffusing and the algorithm may result in false detection. Figure 5 is the result based on the definition of "entropy rise" in Ref. [4]. Here, we modify the expression of the absolute value instead of H_z because "entropy rise" reflects the varying scope of local entropy. We can see from Fig. 5 that the target appears in the position of minimum H_z, not maximum H_z. A method of normalization was introduced to modify the inappropriate aspect[4]:

$$\hat{H} = H/\log(n+1), \tag{5}$$

$$\hat{H}_f = \left[H_f - 1/(n+1)\right] \times \frac{n+1}{n} = \frac{(n+1)H_f - 1}{n} \quad . \tag{6}$$

The normalization method may eliminate the effect of the number of elements of local window. Figure 6 is the result which is not very obvious since it can detect the position of the target. According to the definition of $\hat{H}$ and $\hat{H}_f$, we find that both H and H_f represent local entropy, and the difference between them is their number of elements.

From Eq. (3), we find that H_f is a linear combination with p_{ij}^2. The weight coefficient is equal to 1. It actuates us to rewrite the equation again and revise the

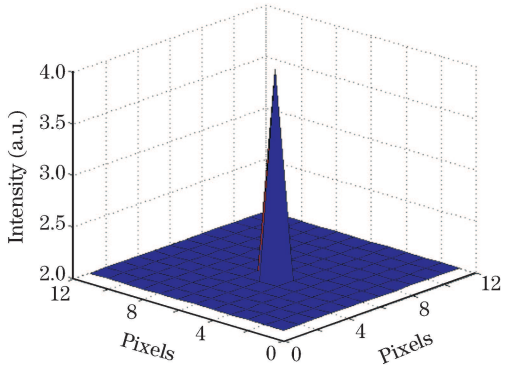

Fig. 3. Original image.

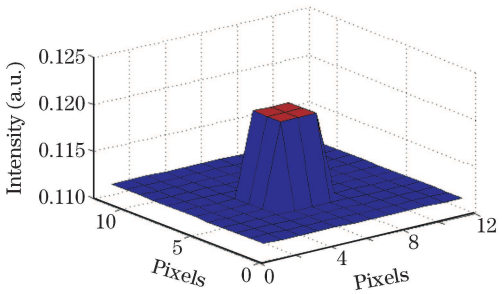

Fig. 4. Result according to Ref. [3].

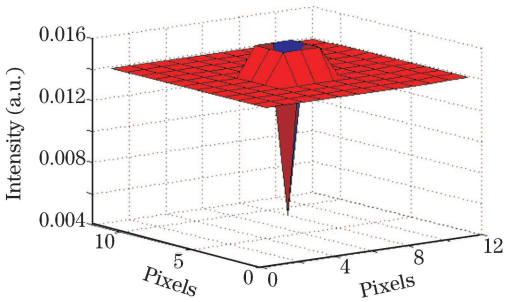

Fig. 5. Result without normalization according to Ref. [3].

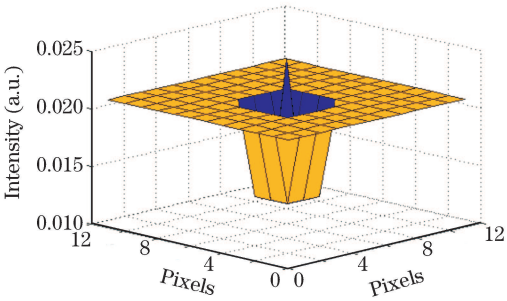

Fig. 6. Result with normalization according to Ref. [3].

weight coefficient. Now we take a new weight coefficient α in the center point:

$$H_f = \sum_{(i,j)\in(M,N)} p_{ij}^2 = \sum_{i\neq j} p_{ij}^2 + \alpha p_{ii}^2 \quad . \tag{7}$$

The coefficient α can be adjusted in the experiments.

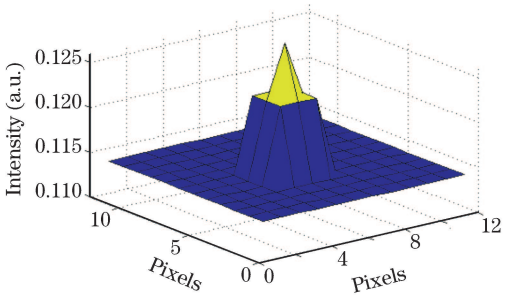

Fig. 7. Result according to modified local entropy.

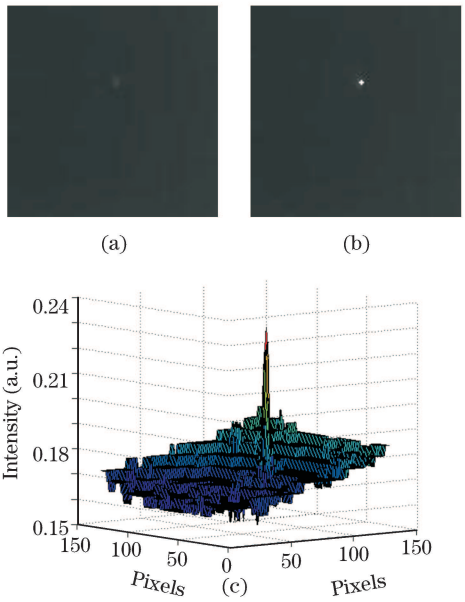

Fig. 8. Small target detection experiment of infrared image under sea-sky background. (a) Original infrared image under uniform background; (b) detecting result based on the modified local entropy; (c) 3D image of the modified local entropy.

Fig. 9. Original infrared images under sea-sky background.

In our experiments, $\alpha > 1$ if the intensity of target is greater than others, and $\alpha < 1$ contrarily. Now we call H_f as the modified local entropy. It cannot only overcome the appearance of target range diffusion, but also avoid some inaccurate conclusions as Ref. [4]. The same conclusion can also be deduced in Fig. 7. From Fig. 7, it can be seen that the position of target is successfully detected and the result is more obvious than the result in Fig. 6.

We performed experiments to further describe the modified local entropy method. Figure 8 is the experimental result of small infrared target under uniform

(a) (b) (c)

Fig. 10. Target detection results of the continuous frames based on EMD and modified local entropy corresponding to Figs. 9(a)−(c).

background, where the size of the original image is 128×128, the window of modified local entropy is 3×3. From Fig. 8, the entropy of background texture is relatively uniform, but in the target scope, it is obviously increscent. So the small target is segmented feasibly by the modified entropy proposed in this letter.

The small target detection is very difficult under the complicated background of infrared image. The general method is suppressing the background of the image and segmenting the target using the threshold. The algorithm based on EMD can decompose the image into different IMFs and the residue, which may be looked as the approximation to the background of the image. Therefore, if the background is subtracted from the original image, it can attain the goal to suppress the background. A result will increase the signal-to-noise ratio (SNR) of the image. It provides a possible way to detect the small target based on the modified local entropy method.

To test the pros and cons of EMD and modified local entropy algorithm in small target detection under complex background of infrared images, we have done a large number of computer simulations. All of those images are under complex sea-sky background, and the SNRs are very low. The experimental procedures are as follows: firstly, suppress the background of the infrared image based on EMD method; secondly, segment the target using a threshold based on the modified entropy method. Serial pictures of 96 frames have been done based on the proposed method, and the size each picture is 128×128. Figure 9 shows three continuous frames with small targets for detection, and Fig. 10 shows the detection results. Through an analysis of the results from Fig. 10, we can conclude that the EMD method really adapts to detect small targets under complex sea-sky background, the proposed algorithm can detect small infrared targets by suppressing the image background based on EMD method and lead to the self-adaptable segmentation threshold based on the modified local entropy.

In conclusion, a new algorithm is put forward for detecting small target under complex background of infrared image based on EMD and modified local entropy. Based on the experimental results, this method can effectively and quickly identify small infrared targets. EMD method is based on the data itself, and therefore it has a good adaptability. The modified local entropy reflects the degree of changes in the intensity of gray level. The initial results are very encouraging and promising. In a word, this new method would really help to isolate noise from airborne gravity data and detect meaningful geological information that might have been masked by noises.

This work was supported in part by the National Natural Science Foundation of China for Young Scholars under Grant No. 40801164.

References

1. L. He, Q. Pan, W. Di, and Y. Zhao, Acta Opt. Sin. (in Chinese) **27,** 2155 (2007).
2. Z. Guan, Q. Chen, G. Gu, and W. Qian, Acta Opt. Sin. (in Chinese) **28,** 1496 (2008).
3. G. Wang, J. Tian, and J. Liu, Infrared and Laser Eng. (in Chinese) **29,** (4) 26 (2000).
4. B. Zhou, Y. Wang, L. Sun, and Y. He, Acta Photon. Sin. (in Chinese) **37,** 381 (2008).
5. N. E. Huang, Z. Shen, S. R. Long, M. C. Wu, H. H. Shih, Q. Zheng, N.-C. Yen, C. C. Tung, and H. H. Liu, Proc. Roy. Soc. London A, **454,** 903 (1998).
6. Y. Barniv, IEEE Trans. Aerospace Electron. Syst. **21,** 144 (1985).
7. S. D. Blostein and T. S. Huang, IEEE Trans. Signal Processing **39,** 1611 (1991).
8. P. Flandrin, G. Rilling, and P. Goncalves, IEEE Signal Process. Lett. **11,** 112 (2004).
9. P. Flandrin, P. Goncalves, and G. Rilling, in *Proceedings of the European Signal Processing Conference (EUSIPCO'04)* 1581 (2004).
10. C. Damerval, S. Meignen, and V. Perrier, IEEE Signal Processing Lett. **12,** 701 (2005).